

The giant oyster *Hyotissa hyotis* from the northern Red Sea as a decadal-scale archive for seasonal environmental fluctuations in coral reef habitats

J. Titschack · M. Zuschin · C. Spötl ·
C. Baal

Received: 17 November 2009 / Accepted: 22 July 2010 / Published online: 14 August 2010
© Springer-Verlag 2010

Abstract This study explores the giant oyster *Hyotissa hyotis* as a novel environmental archive in tropical reef environments of the Indo-Pacific. The species is a typical accessory component in coral reefs, can reach sizes of tens of centimetres, and dates back to the Late Pleistocene. Here, a 70.2-mm-long oxygen and carbon isotope transect through the shell of a specimen collected at Safaga Bay, northern Red Sea, in May 1996, is presented. The transect runs perpendicularly to the foliate and vesicular layers of the inner ostracum near the ligament area of the oyster. The measured $\delta^{18}\text{O}$ and $\delta^{13}\text{C}$ records show sinusoidal fluctuations, which are independent of shell microstructure. The $\delta^{13}\text{C}$ fluctuations exhibit the same wavelength as the $\delta^{18}\text{O}$ fluctuations but are phase shifted. The $\delta^{18}\text{O}$ record reflects the sea surface temperature variations from 1957 until 1996, possibly additionally influenced by the local

evaporation. Due to locally enhanced evaporation in the semi-enclosed Safaga Bay, the $\delta^{18}\text{O}_{\text{seawater}}$ value is estimated at 2.17‰, i.e., 0.3–0.8‰ higher than published open surface water $\delta^{18}\text{O}$ values (1.36–1.85‰) from the region. The mean water temperature deviates by only 0.4°C from the expected value, and the minimum and maximum values are 0.5°C lower and 2.9°C higher, respectively. When comparing the mean monthly values, however, the sea surface temperature discrepancy between reconstructed and global grid datasets is always <1.0°C. The $\delta^{13}\text{C}$ signal is weakly negatively correlated with regional chlorophyll a concentration and with the sunshine duration, which may reflect changes in the bivalve's respiration. The study emphasises the palaeogeographic context in isotope studies based on fossils, because coastal embayments might not reflect open-water oceanographic conditions.

Keywords Molluscs · Bivalves · Stable isotopes · Environmental archive

Communicated by Geology Editor Prof. Bernhard Riegl

J. Titschack (✉)
MARUM, Center for Marine Environmental Sciences,
University of Bremen, Leobener Strasse,
28359 Bremen, Germany
e-mail: titschack@uni-bremen.de

J. Titschack
Senckenberg am Meer, Abteilung für Meeresforschung,
Südstrand 40, 26382 Wilhelmshaven, Germany

M. Zuschin · C. Baal
Department of Palaeontology, University of Vienna,
Althanstrasse 14, 1090 Vienna, Austria

C. Spötl
Department of Geology and Palaeontology, University
of Innsbruck, Innrain 52, 6020 Innsbruck, Austria

Introduction

Climate models require high-resolution, temporarily equidistant oceanographic data that cover long time periods (Schöne et al. 2004; Wanamaker et al. 2007). Often these models rely on high-resolution palaeoenvironmental recorders. In tropical climates, corals are commonly used due to their longevity and high growth rate (e.g., Klein et al. 1997; Felis et al. 2004; Rimbu et al. 2006; Al-Rousan et al. 2002). In contrast, bivalves are rarely considered in the tropics, and studies are mostly restricted to the giant clams (e.g., Jones et al. 1986; Romanek and Grossman 1989; Aharon 1991; Watanabe and Oba 1999; Watanabe et al. 2004; Elliot et al. 2009). In temperate waters,

however, bivalves represent the most widely used environmental archives (Krantz et al. 1987; Hickson et al. 1999; Schöne et al. 2002, 2003a, 2005b; Carré et al. 2005; Gillikin et al. 2005; Scource et al. 2006; Wanamaker et al. 2007, 2008a, b; Goman et al. 2008; Butler et al. 2009a, b). Some bivalves are among the longest lived animals (up to 400 years; Schöne et al. 2005b; Wanamaker et al. 2008b; Wisshak et al. 2009) and potentially record, as do tropical corals, the ambient seasonal environmental conditions over decades to centuries (Schöne et al. 2005b; Strom et al. 2005; McConnaughey and Gillikin 2008; Wanamaker et al. 2008a; Butler et al. 2009a). Specimens with overlapping lifespans can be combined to form so-called master chronologies (Jones et al. 1989; Schöne 2003; Scource et al. 2006; Butler et al. 2009a, b).

This study investigates the potential of tropical oysters from Safaga Bay, Red Sea, as seasonal environmental archives. For this purpose, the microstructure development and the high-resolution oxygen and carbon stable isotope records of the gryphaeid oyster *Hyotissa hyotis* (Linnaeus, 1758) is studied. The latter dataset is compared with environmental datasets. *H. hyotis* belongs to the subfamily Pycnodonteinae. The geographical extension of *H. hyotis* covers the tropical and subtropical waters of the Indo-Pacific (e.g., Zuschin and Oliver 2003a, b). Recently, it was introduced to the western Atlantic (Bieler et al. 2004). The species is a typical accessory component in fossil and recent coral reefs and has been present on the Red Sea coast since the Late Pleistocene (Crame 1986; Zuschin et al. 2001). *H. hyotis* is exceptional in that it can grow tens of centimetres in size.

Red Sea

The Red Sea is a deep, channel-like, semi-enclosed, desert-surrounded, evaporitic basin (Edwards 1987). The estimated net evaporation is about 200 cm/year (Ahmed and Sultan 1987). In the northern Red Sea, evaporation is not a simple function of temperature. According to Eshel and Heavens (2007), the land–sea thermal contrast is the main physical parameter affecting the hydrological cycle: it maximises evaporation during winter and minimises it during summer. The mean annual rainfall is negligible, and the Red Sea rainfall catchment area is small (Felis et al. 2004). Edwards (1987) reviewed extensive Red Sea temperature sources and concluded that throughout the Red Sea the lowest surface temperatures occur in February and the highest values in August (northern Red Sea: February 22–23°C, August 27–28°C). Coastal waters, however, can significantly deviate from the open ocean monthly mean temperatures (Edwards 1987; Medio et al. 2000).

Sampling location

The northern Bay of Safaga (Fig. 1) is a shallow-water area with a structured bottom topography extending down to below 50 m (Riegl and Piller 1997; Zuschin and Hohegger 1998; Grill and Zuschin 2001). Temperature and salinity show no obvious depth gradient due to complete water mixing in the bay (Piller and Pervesler 1989; Helal and El-Wahab 2004).

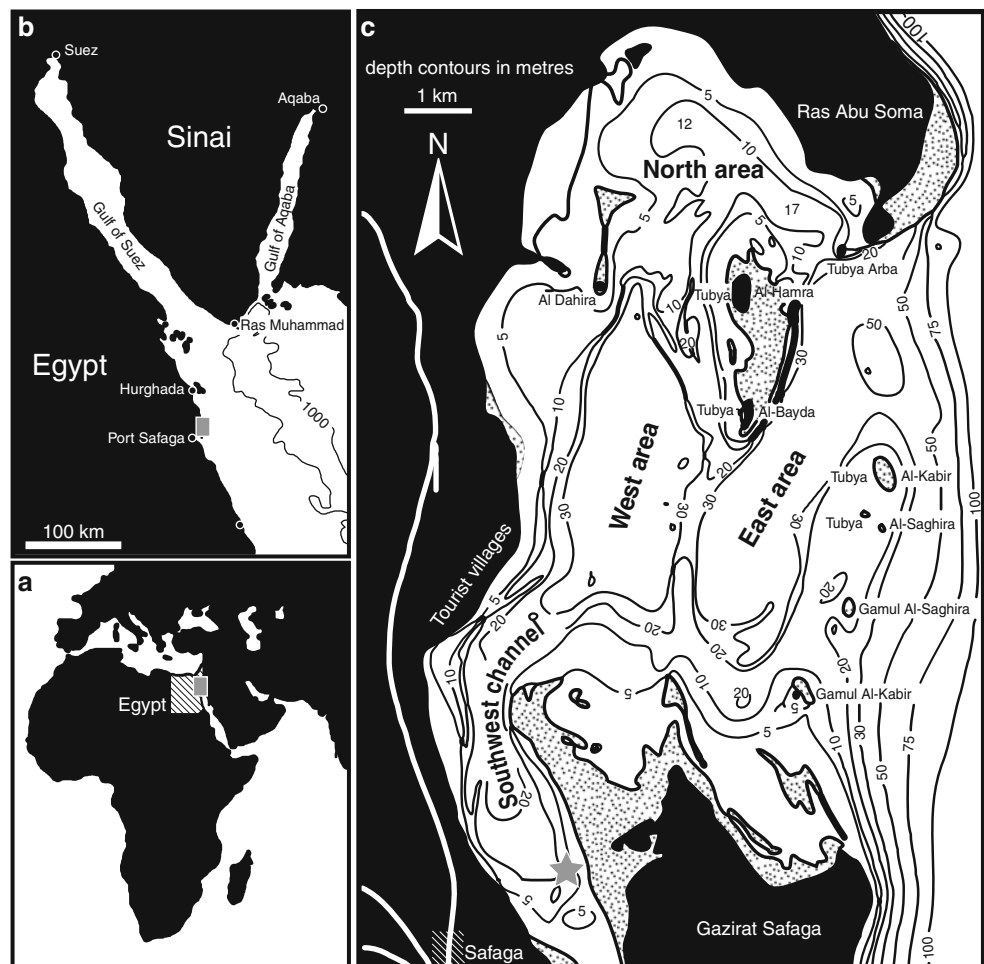
One living specimen of *H. hyotis* was collected in May 1996 from a shallow-water site (26.77°N, 33.95°E, 6 m water depth; Fig. 1) at the southern tip of the northern Bay of Safaga, where it was attached to a dead and degraded massive coral colony (Fig. 2 in Zuschin and Baal 2007). The dorsal–ventral size of its lower (left) valve exhibits a length of 29 cm (Fig. 2).

Methods

All analyses were obtained from a slab positioned through the resilifer (central ligament) and along the maximal growth direction (Fig. 2). For sclerochronological and microstructural analysis, three methods were applied: (1) high-resolution scanning of the longitudinal section with a conventional flat-bed scanner, (2) transmission light microscopy of thin sections using a WILD M400 microscope, and (3) JEOL 6400 scanning electron microscope (SEM). For the SEM, sections were polished, treated with 10% EDTA (ethylenediaminetetraacetic acid) for 90 s, and subsequently gold coated with the sputter coater BIO-RAD SC 500. The foliate and vesicular microstructure alternations along the isotope transect were counted, and their thicknesses measured.

For oxygen and carbon isotope measurements, a profile parallel to the growth direction in the proximal inner ostracum was selected (Fig. 2). The sample powders were milled with a Merchantek Micro Mill (NewWave). Two hundred and sixty tracks with a length of about 4 mm and a distance between two tracks of about 270 µm were set with the Micro Mill System Software. Tracks were drilled 300 µm deep, and about 70–100 µg sample powder was recovered from each. Subsequently, samples were prepared using an online carbonate preparation system (GasBench II) interfaced with a ThermoFisher DeltaplusXL isotope ratio mass spectrometer operating in continuous-flow mode. Standardisation was accomplished using the NBS19 standard, and scale conversion was repeatedly checked using NBS18 (Spötl and Vennemann 2003). No drift occurred during these analyses. Results are reported relative to the Vienna Pee Dee Belemnite (VPDB) standard. Reproducibility was checked by replicate analysis of laboratory standards and is better than ±0.06‰ for δ¹³C and

Fig. 1 **a, b** Location of the study area on the western margin of the northern Red Sea. **c** Bathymetric map of the study area (modified after Piller and Pervesler 1989). Grey star indicates collection site of *Hytissa hyotis*. Dense stippled fields are intertidal areas



better than $\pm 0.08\text{‰}$ for $\delta^{18}\text{O}$ (1σ). Four samples did not contain enough material for a successful isotope measurement.

To compare the isotope record to environmental variables obtained from satellite surveys and weather station records, and to estimate growth rates, the isotope data were converted from a distance scale to an absolute time scale by tying the $\delta^{18}\text{O}$ maxima and minima of the oyster (hereafter referred to as $\delta^{18}\text{O}_{\text{oyster}}$) to the dates of the minima and maxima of the monthly sea surface temperature (SST) record, respectively. This procedure started at the inner surface of the shell (precipitated shortly before sampling) with the sampling year, and continued from this surface backward in time (see also Omata et al. 2005). Thereby, the difference between maxima and minima generally exceeded 0.7‰ . Only at 13–15 mm, 26–28 mm, and 52–55 mm were the fluctuations with a difference $< 0.7\text{‰}$ considered to be caused by the seasonal SST oscillations because, otherwise, unrealistically high growth rates would have to be assumed. The dates of samples between maxima and minima were interpolated linearly

assuming a constant growth rate between the seasons (indicated by the rather sinusoidal-shaped fluctuations of the $\delta^{18}\text{O}_{\text{oyster}}$ record, especially from 0 to 35 mm). Each year is defined by at least 3 values (only the case for 4 years) and up to 12 values (mean 6). To compare the measured isotope record with environmental datasets, both the $\delta^{18}\text{O}_{\text{oyster}}$ values were linearly interpolated to the dates of the monthly environmental datasets (to calculate monthly mean values), and the monthly environmental datasets were interpolated to the interpolated dates of the $\delta^{18}\text{O}_{\text{oyster}}$ record (for testing the correlation between the datasets). The uncertainty of the age model is estimated to be approximately 3 months in any given year, due to the relatively high variability of measurements that define a year (3–12). Shell growth rate estimations are based on this age model. Yearly growth rates were computed by calculating the wavelength of every year, taking the interpolated 1st January as fix points. A synthetic calcite $\delta^{18}\text{O}$ record (hereafter referred to as $\delta^{18}\text{O}_{\text{predicted}}$), assuming isotopic equilibrium with seawater, was calculated by solving temperature equations for $\delta^{18}\text{O}_{\text{predicted}}$ instead of

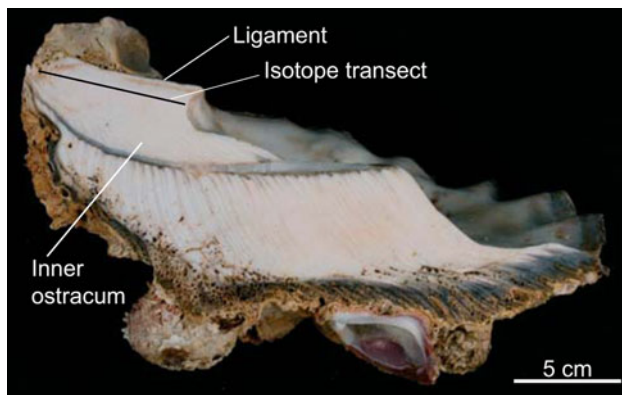


Fig. 2 The left (attached) valve of the oyster sectioned from dorsal to ventral through the resilifer and parallel to the maximum growth direction. The isotopic composition was analysed along a transect perpendicular to skeletal growth increments of the inner ostracum near the ligament area

temperature. For this purpose, three equations of Anderson and Arthur (1983) and Wanamaker et al. (2007, Eqs. 4, 5) were compared.

Two different modes of estimating the $\delta^{18}\text{O}_{\text{seawater}}$ were used: (1) a fixed $\delta^{18}\text{O}_{\text{seawater}}$ value and (2) $\delta^{18}\text{O}_{\text{seawater}}$ values calculated from the $\delta^{18}\text{O}_{\text{seawater}}$ –sea surface salinity (SSS) relationship (hereafter referred to as $\delta^{18}\text{O}_{\text{seawater(SSS)}}$) for the Red Sea determined by LeGrande and Schmidt (2006). When using published $\delta^{18}\text{O}_{\text{seawater}}$ values (1.85‰, Andrić and Merlivat 1989; 1.36‰, Gansen and Kroon 1991) or the $\delta^{18}\text{O}_{\text{seawater(SSS)}}$, there was a significant offset between $\delta^{18}\text{O}_{\text{predicted}}$ and the $\delta^{18}\text{O}_{\text{oyster}}$ record. Therefore, the fixed $\delta^{18}\text{O}_{\text{seawater}}$ as well as a constant, added to the $\delta^{18}\text{O}_{\text{seawater(SSS)}}$, were varied between 2.0–2.5‰ and 0.9–1.0‰ in 0.01 and 0.001‰ steps, respectively, until the maximal absolute error between the $\delta^{18}\text{O}_{\text{oyster}}$ and $\delta^{18}\text{O}_{\text{predicted}}$ record was minimal ($\delta^{18}\text{O}_{\text{predicted}}$ was taken as predictand). Regression lines, coefficient of determination, and *P* values were calculated with SigmaPlot. The Spearman rank order correlation was applied only for the SSS– $\delta^{18}\text{O}$ and SST–SSS comparison because the data failed the normality test (Shapiro–Wilk).

Environmental datasets

Environmental datasets used in this study include SST, SSS, daily sunshine, and chlorophyll *a* (Fig. 3). Monthly mean SSTs were extracted from the HadISST 1.1 dataset of the UK Meteorological Office (2006) from 27°N and 34°E (December 1956 to April 1996). Piller and Pervesler (1989) provided measured monthly mean SSTs from Safaga Bay with 24.7°C in May 1986, 26.9°C in November 1986, 22.8°C in February 1987, and 28.4°C in July 1987,

suggesting an annual range of about 22–29°C. Measurements close to the oyster’s living site yielded 23.4°C in April 1986 and 27.7°C in July 1987.

Modelled monthly mean SSSs were obtained from CARTON-GIESE SODA version 2.0.2-4 for 26.75°N and 33.75°E (5 m water depth; 1958–2001; Carton and Giese 2008). Direct SSS measurements from Safaga Bay exhibit a range of 41–45‰ (May 1986: 42.7‰; November 1986: 43.4‰; February 1987: 41.7‰; July 1987: 44.5‰; Piller and Pervesler 1989).

Daily sunshine hours for 27.12°N and 31.10°E from 1980 to 1993 were obtained from the World Radiation Data Centre (<http://wrdc-mgo.nrel.gov/>).

Monthly mean chlorophyll *a* data for the Safaga region (26.67°N and 34.17°E) was obtained from the NASA/SeaWiFS Project (<http://oceancolor.gsfc.nasa.gov/>) from September 1997 to November 2002. Note that the available dataset does not overlap with the lifespan of the collected oyster. Therefore, the chlorophyll *a* dataset is used only for a general comparison of the mean annual chlorophyll *a* fluctuations in the region.

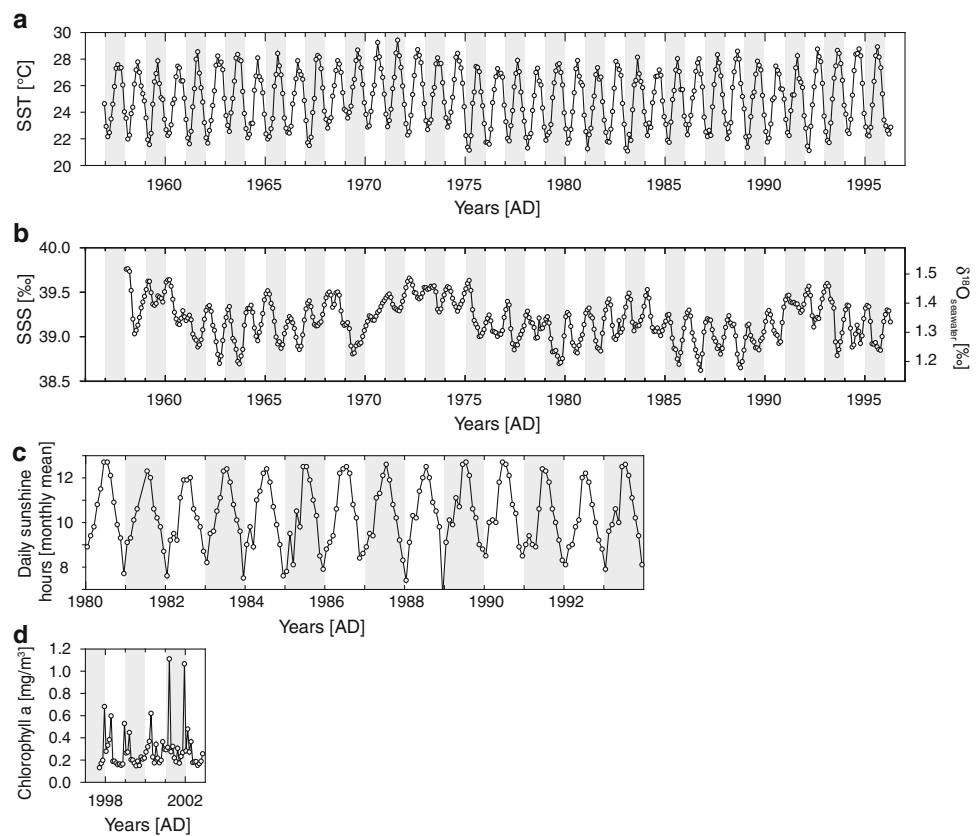
Results

Sclerochronology and microstructure

The outer ligament surface showed alternating convex and concave bands (Fig. 4a, b), whereby the concave bands were associated with clear growth increments in the foliate microstructure close to the ligament (Fig. 4c, d). Altogether, 37 growth band couplets were identified (Fig. 4b).

The inner ostracum consisted of alternating layers with a foliate and a vesicular microstructure; the thickness of these layers varied considerably, ranging from 0.4 to 3.8 mm and from 0.6 to 2.6 mm, respectively (Fig. 4a, c). The annual growth rate within the inner ostracum was estimated to vary between 0.8 and 3.3 mm (mean 1.7 mm; Fig. 5c). The highest growth rates occurred in the early ontogenetic phase from 1960 to 1965 and from 1972 to 1976. Since 1977, the growth rate generally declined (Fig. 5c). No correlation of growth increments in the foliate microstructure close to the ligament with the altering microstructure of the inner ostracum was possible. The significantly higher number of microstructure couplets of foliate and vesicular layers in the inner ostracum (57) compared to the growth increments in the foliate microstructure close to the ligament (37) suggested no direct linkage between them. Petrographic examination of the microstructure revealed no evidence of diagenetic alteration, such as cements or recrystallisation (Fig. 4).

Fig. 3 Environmental data (monthly means) from the Safaga region used in this study (data sources are mentioned in text). **a** Sea surface temperatures. **b** Sea surface salinities. **c** Daily sunshine hours. **d** Chlorophyll a concentrations. Note that chlorophyll a data is only available from September 1997 to November 2002. Vertical, shaded bars indicate uneven years



Stable isotopes

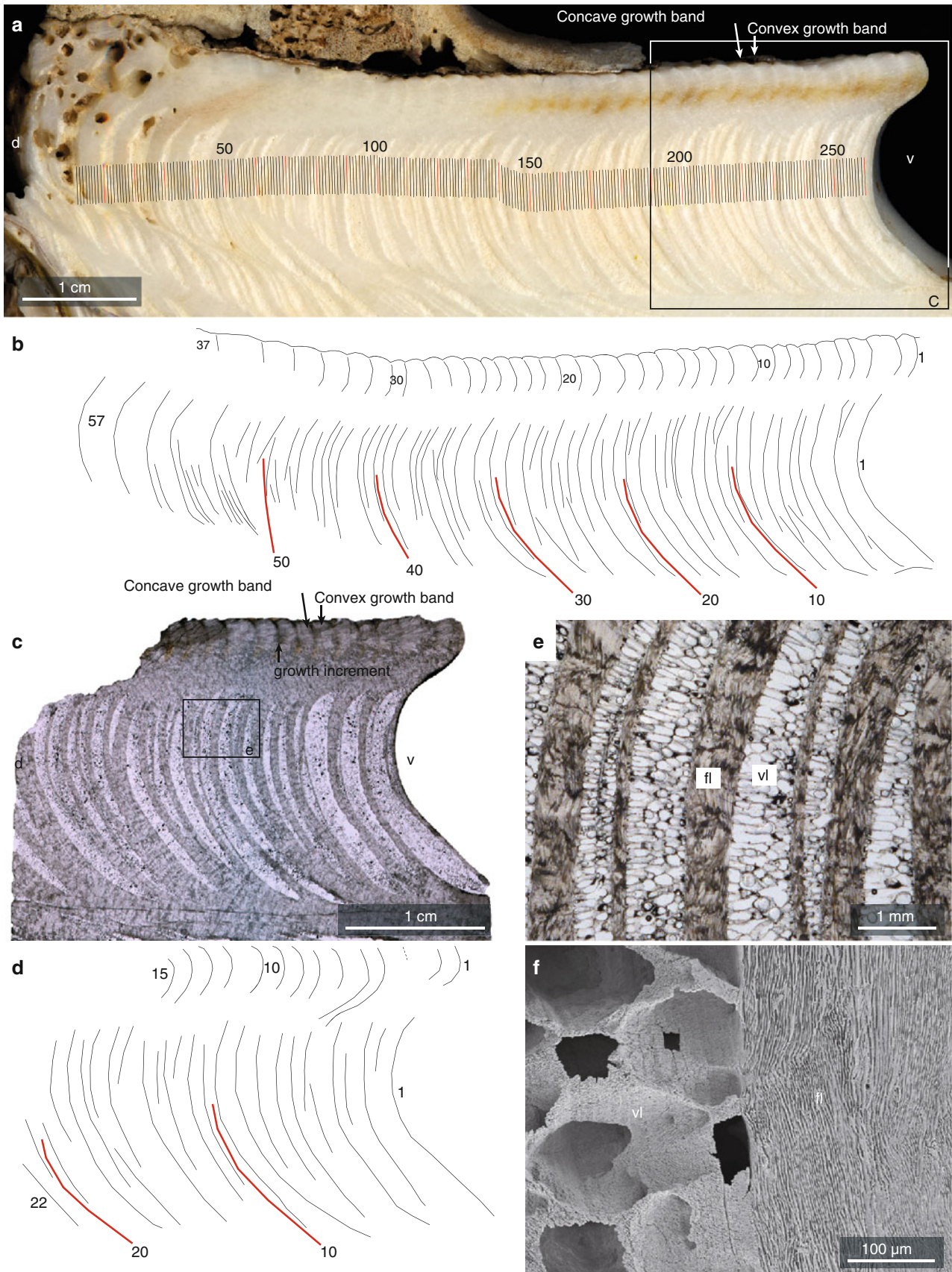
The $\delta^{18}\text{O}$ values varied between -1.19 and 1.23‰ , with a mean of 0.22‰ and a standard deviation (SD) of 0.47‰ . The $\delta^{13}\text{C}$ values varied between 0.54 and 2.2‰ , with a mean of $1.34 \pm 0.35\text{‰}$ (SD; Fig. 5a). $\delta^{13}\text{C}$ correlated only very weakly with $\delta^{18}\text{O}$ (non-significant for monthly mean values) and no difference between the two microstructures was observed (Fig. 6a). Both isotope records exhibited sinusoidal oscillations (Fig. 6b). About 40 of these oscillations were counted in the $\delta^{18}\text{O}_{\text{oyster}}$ record, suggesting that the oyster lived at least from 1957 until 1996 when it was collected.

Comparison of stable isotope data with environmental datasets

The $\delta^{18}\text{O}_{\text{oyster}}$ record correlated negatively with the SST of the region (Fig. 7a). The strong relationship was even more obvious when examining the mean values of each month for the entire data interval (Fig. 7b, c). A very weak (positive) correlation was observed between SSS and $\delta^{18}\text{O}_{\text{oyster}}$ values (Fig. 7d). The SSS oscillations were clearly in-phase with the $\delta^{18}\text{O}_{\text{oyster}}$ fluctuations (Fig. 7e, f).

The three temperature equations, each calculated with a constant and variable $\delta^{18}\text{O}_{\text{seawater}}$ (calculated from the SSS; for details see Table 1 and method section), were used to calculate a $\delta^{18}\text{O}_{\text{predicted}}$ from the SST dataset and were compared with the $\delta^{18}\text{O}_{\text{oyster}}$ record. Best fit was achieved with Eq. 4 of Wanamaker et al. (2007) with a constant $\delta^{18}\text{O}_{\text{seawater}}$ of 2.17‰ (Table 1; Fig. 8). The Anderson and Arthur (1983) temperature equation, however, also showed a good fit with a constant $\delta^{18}\text{O}_{\text{seawater}}$ of 2.36‰ . The

Fig. 4 Microstructures of the studied oyster. **a** Polished slab of the ligament and inner ostracum. Dorsal part of the shell is bioeroded by clionid sponge borings. Position of isotope samples is indicated. Box indicates position of thin section shown in **c**. **b** Sketch of **a** showing the growth banding in the foliate microstructure of the ligament area and foliate and vesicular microstructure couplets in the inner ostracum. The black lines in the foliate microstructure close to the ligament indicate position of growth increments and concave growth bands of the ligament surface, while the black lines in the inner ostracum mark the boundaries between couplets consisting of a vesicular and a foliate layer. **c** Thin section of **a**. Box indicates position of close-up photograph shown in **e**. **d** Sketch of **c**. Black lines are explained in **c**. **e** Close-up photograph of **c**. **f** SEM photograph of foliate and vesicular microstructure. Photographs **e** and **f** exhibit no cements in the pores of the vesicular microstructure or any evidence of recrystallisation. Photographs **c**, **d**, and **e** were inverted to be consistent with photograph **a**. *d* dorsal, *v* ventral, *fl* foliate microstructure, *vl* vesicular microstructure



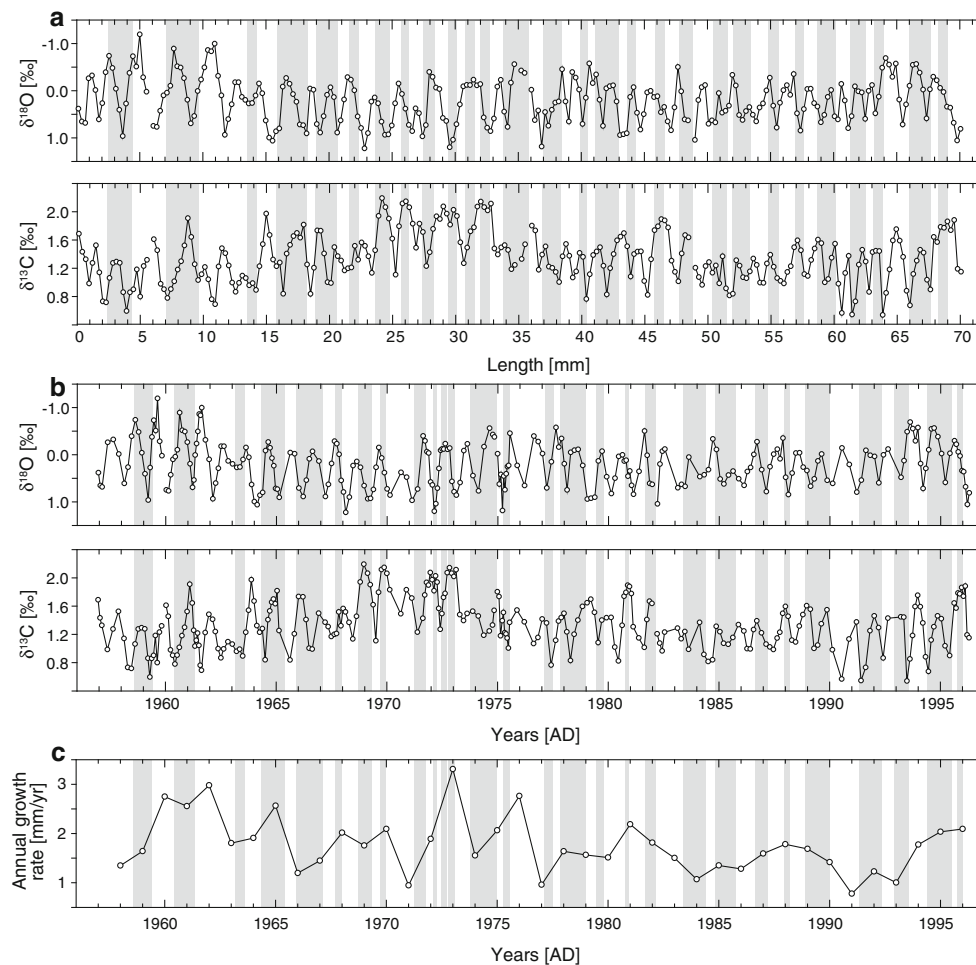
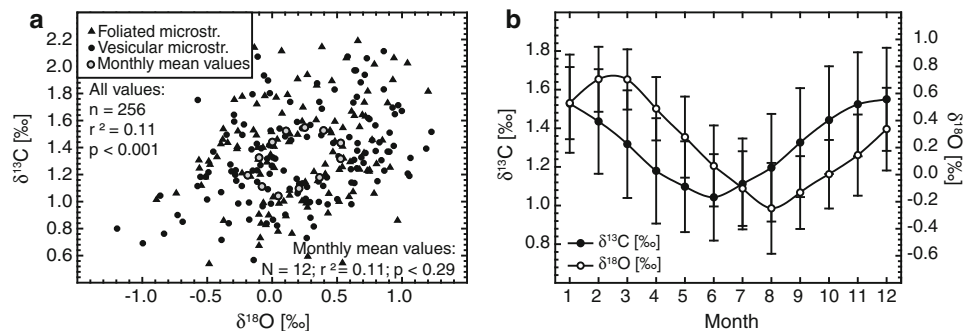


Fig. 5 a Oxygen and carbon isotope data of *Hyotissa hyotis* (location of transect: Fig. 4a). b Isotope data plotted against time. c Annual growth rate of *H. hyotis*, suggesting high growth rates from 1958 to 1977. Vertical shaded bars indicate intervals with a vesicular microstructure

Fig. 6 a Relationship between shell microstructure and isotopic composition. Grey-filled circles Mean values from each month of each year. b Comparison of the $\delta^{18}\text{O}$ and $\delta^{13}\text{C}$ signals using the mean values from each month of each year. Both records show the same wavelength, but the $\delta^{13}\text{C}$ signal precedes the $\delta^{18}\text{O}$ signal by 2 months



$\delta^{18}\text{O}_{\text{oyster}}$ exhibited a maximal absolute error from the $\delta^{18}\text{O}_{\text{predicted}}$, calculated with the two above-mentioned equations, of 0.95‰ and a mean absolute error of 0.27‰ (Table 1). Compared with the amplitude of $\delta^{18}\text{O}_{\text{predicted}}$ that of $\delta^{18}\text{O}_{\text{oyster}}$ was reduced in most years (Fig. 7b).

The minimum, maximum, and mean $\delta^{18}\text{O}_{\text{oyster}}$ values suggested corresponding SSTs of 20.6°C (23.1°C; temperatures in parentheses reflect monthly mean values;

Table 2), 32.3°C (27.7°C), and 25.4°C (25.4°C), respectively (calculated with Eq. 4 of Wanamaker et al. 2007, $\delta^{18}\text{O}_{\text{seawater}} = 2.17\text{‰}$). The mean value deviated by only 0.4°C (0.4°C) from the expected value of 25.0°C (25.0°C) generated from the SST dataset, which was within the analytical error. The minimum was 0.5°C colder (1.0°C warmer when compared with the monthly mean temperatures) than the expected 21.1°C (22.1°C), and the

Fig. 7 **a** Crossplot of the local sea surface temperatures (SSTs) and the $\delta^{18}\text{O}_{\text{oyster}}$ record. **b** Mean values of the monthly SSTs, $\delta^{18}\text{O}_{\text{predicted}}$, and interpolated $\delta^{18}\text{O}_{\text{oyster}}$ record for each month and their standard deviation (SD) for the entire data interval. **c** Crossplot of the monthly mean local SSTs and the mean monthly $\delta^{18}\text{O}_{\text{oyster}}$. **d** Crossplot of the local sea surface salinities (SSSs) and the $\delta^{18}\text{O}_{\text{oyster}}$. **e** Mean values of the monthly SSSs and $\delta^{18}\text{O}_{\text{oyster}}$ values for each month and their SD for the entire data interval. **f** Crossplot of the monthly mean local SSSs and the mean monthly $\delta^{18}\text{O}_{\text{oyster}}$ record

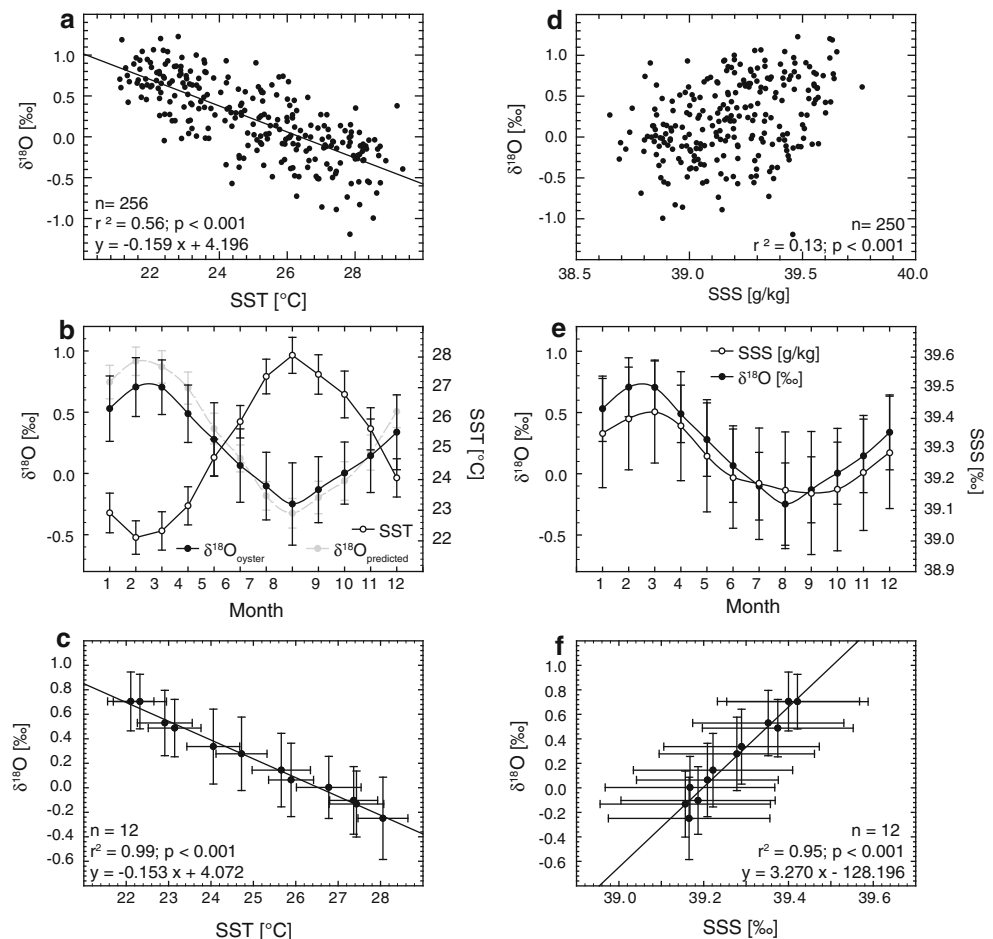


Table 1 Comparison between the measured $\delta^{18}\text{O}_{\text{oyster}}$ record and $\delta^{18}\text{O}_{\text{predicted}}$ record calculated from sea surface temperature (extracted from HadISST 1.1 dataset) and various temperature equations

Temperature equation	$\delta^{18}\text{O}_{\text{seawater}}$ (‰)	Maximal absolute error**	Mean absolute error**
Wanamaker et al. (2007, Eq. 5)	$\delta^{18}\text{O}_{\text{seawater(SSS)}} + 0.925^*$	0.97	0.30
Wanamaker et al. (2007, Eq. 5)	2.28	0.99	0.29
Wanamaker et al. (2007, Eq. 4)	$\delta^{18}\text{O}_{\text{seawater(SSS)}} + 0.795^*$	0.96	0.28
Wanamaker et al. (2007, Eq. 4)	2.17	0.95	0.27
Anderson and Arthur (1983)	$\delta^{18}\text{O}_{\text{seawater(SSS)}} + 0.985^*$	0.96	0.29
Anderson and Arthur (1983)	2.36	0.95	0.27

* $\delta^{18}\text{O}_{\text{seawater}}$ is calculated with the LeGrande and Schmidt (2006) $\delta^{18}\text{O}_{\text{seawater}}$ – salinity equation: $\delta^{18}\text{O}_{\text{seawater(SSS)}} = 0.31 \times \text{salinity} - 10.81$ and sea surface salinity data extracted from CARTON-GIESE SODA version 2.02-4. A correction was added to compensate the increased evaporation in Safaga Bay. ** For the calculation of the absolute error, the $\delta^{18}\text{O}_{\text{predicted}}$ values were taken as predictand

maximum value was 2.9°C warmer (0.4°C colder compared with the monthly mean) than the expected 29.4°C (28.1°C). Hence, the reconstructed SSTs might exhibit an absolute error of up to 3°C versus expected values, but monthly mean values were much more reliable (absolute error < 1°C; Table 2).

The $\delta^{13}\text{C}_{\text{oyster}}$ fluctuations oscillated at the same wavelength as the $\delta^{18}\text{O}_{\text{oyster}}$ signal but were phase shifted, i.e.,

they preceded the $\delta^{18}\text{O}_{\text{oyster}}$ signal by 2 months (Fig. 6b; estimated from shifts in the minima and maxima of the sinusoidal annual fluctuations). The regional chlorophyll a dataset exhibited two plankton blooms, with maxima in December and March. Bloom intensity, however, varied from year to year, and in some years only one bloom occurred (Figs. 3d, 9a). Comparing the chlorophyll a dataset with the $\delta^{13}\text{C}_{\text{oyster}}$ signal showed a non-significant, very weak

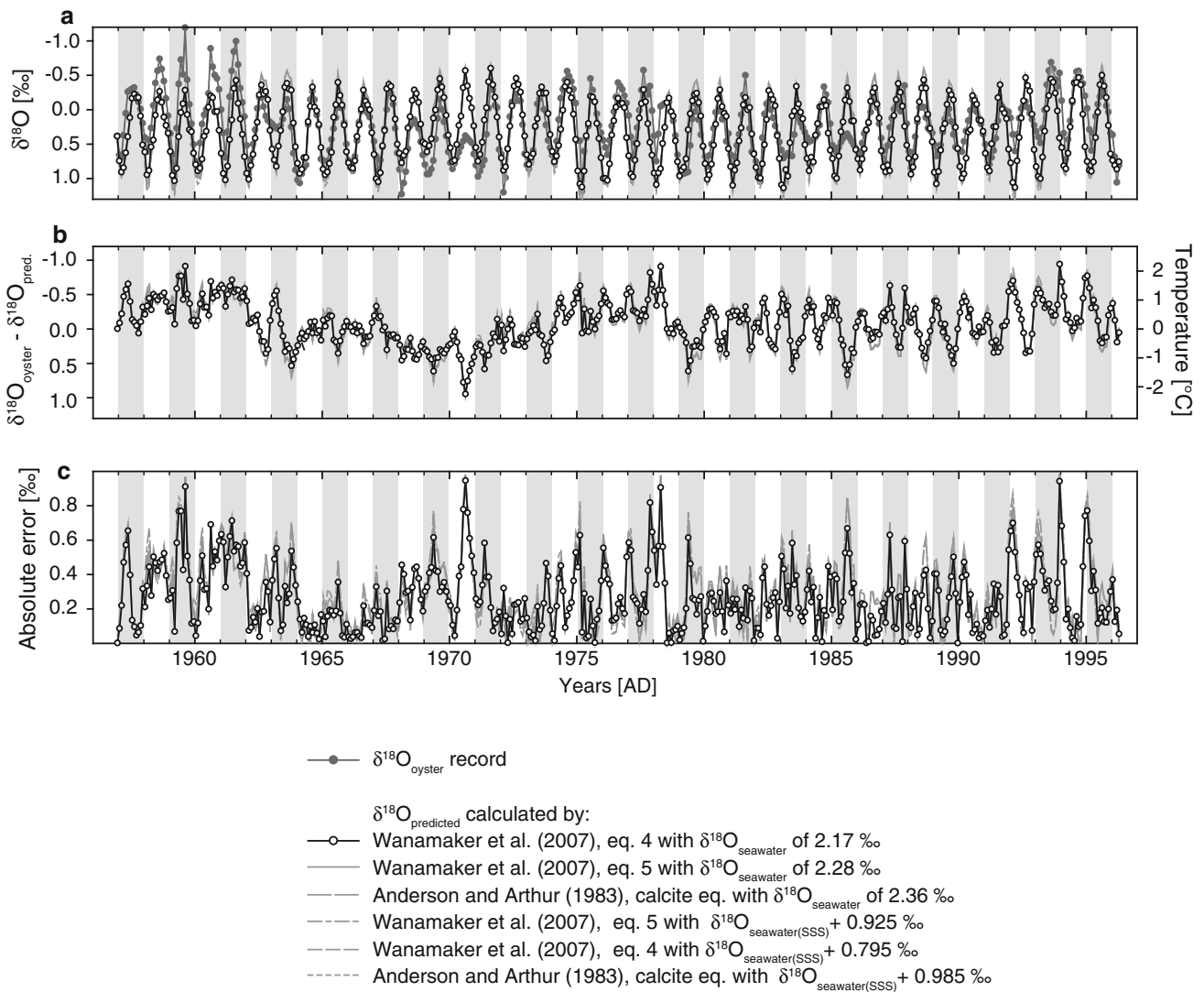


Fig. 8 **a** Comparison of the $\delta^{18}\text{O}_{\text{oyster}}$ record with the $\delta^{18}\text{O}_{\text{predicted}}$, calculated from the sea surface temperatures dataset using three temperature equations with constant and variable $\delta^{18}\text{O}_{\text{seawater}}$ values.

b Difference between $\delta^{18}\text{O}_{\text{oyster}}$ and $\delta^{18}\text{O}_{\text{predicted}}$. **c** Absolute error between $\delta^{18}\text{O}_{\text{oyster}}$ and $\delta^{18}\text{O}_{\text{predicted}}$. Vertical, shaded bars indicate uneven years

correlation (Fig. 9b), but the change from increasing to decreasing $\delta^{13}\text{C}_{\text{oyster}}$ values coincided with the December plankton bloom, and decreasing $\delta^{13}\text{C}_{\text{oyster}}$ values occurred until the end of the March bloom (Fig. 9a). Comparing the $\delta^{13}\text{C}_{\text{oyster}}$ data with the mean monthly sunshine duration (Fig. 9c) showed a negative correlation (Fig. 9d, f). Furthermore, both oscillations are in-phase (Fig. 9e).

Discussion

Bivalves are used for environmental reconstructions in a range of environments. These include fully marine tropical waters (Jones et al. 1986; Romanek and Grossman 1989; Aharon 1991; Surge and Walker 2006; Elliot et al. 2009),

temperate systems (Krantz et al. 1987; Hickson et al. 1999; Schöne et al. 2002, 2003a, 2004, 2005b; Takesue and van Geen 2004; Carré et al. 2005; Gillikin et al. 2005; Wanamaker et al. 2007, 2008b; Goman et al. 2008), brackish (Kirby et al. 1998; Putten et al. 2000; Surge et al. 2003), freshwaters (Dunca et al. 2005; Geist et al. 2005; Schöne et al. 2005a), and methane seeps (Lietard and Pierre 2008). Among oysters, several studies concentrated on temperate, shallow estuarine waters (e.g., Hong et al. 1995; Kirby et al. 1998; Andrus and Crowe 2000; Kirby 2000; Surge et al. 2001, 2003; Lartaud et al. 2010a), and on deep waters (Wisshak et al. 2009). The herein-studied tropical oyster *H. hyotis* provides an environmental archive in coral reefs and might function as useful alternative to corals and tridacnids in the region of its geographical extension, the

Table 2 Comparison of monthly mean temperatures obtained from the oxygen isotope record and the sea surface temperature

Month	$T_{\delta^{18}\text{O}_{\text{oyster}}} \text{ (}^\circ\text{C)}^*$	SST ($^\circ\text{C}$)	Maximal absolute error ($^\circ\text{C}$)
January	23.9	22.9	1.0
February	23.1	22.1	1.0
March	23.1	22.3	0.8
April	24.1	23.1	1.0
May	25.1	24.7	0.4
June	26.2	25.9	0.3
July	27.0	27.4	0.4
August	27.7	28.1	0.4
September	27.1	27.4	0.3
October	26.5	26.8	0.3
November	25.8	25.7	0.1
December	24.9	24.1	0.8

* $T_{\delta^{18}\text{O}_{\text{oyster}}} \text{ (}^\circ\text{C)}$ are based on the temperature Eq. 4 of Wanamaker et al. (2007) with a $\delta^{18}\text{O}_{\text{seawater}}$ value of 2.17‰

Quaternary Indo-Pacific (for references see Zuschin and Baal 2007). Large and long-lived oysters, such as *H. hyotis*, provide several advantages over other environmental archives. They (1) are fixosessile, which promotes fossilisation in life position and allows the integration of environmental information extracted from the layer in which they are fossilised and vice versa, (2) grow slowly, thus reducing kinetic effects (McConnaughey 1989), (3) lack symbionts, which results in a simpler biochemical system with respect to metabolic effects when compared to symbiotic organisms, e.g., zooxanthellate corals and tridacnid bivalves, and (4) have shells composed of low-Mg calcite, which enhances the preservation potential of geochemical signals during diagenesis compared to aragonitic skeletons.

Sclerochronology and microstructure

The sclerochronological and microstructural observations are from the inner ostracum and ligament area of a longitudinal section (Figs. 2, 4). The 37 convex–concave alternations, with growth increments in the foliate microstructure of the concave bands of the ligament surface, closely matches the age of the oyster reconstructed from the stable isotope record (i.e., 40 years; Figs. 4, 5a, b). Consequently, they are interpreted as annual. However, age estimates based on counting the growth bands of the ligament surface must be treated with caution because the counts might be highly affected by secondary processes, such as abrasion or bioerosion (left basal part of Fig. 4a). Therefore, it is suggested to combine the ligament surface observation with growth increment data from the foliate microstructure close to the ligament, a site which is less sensitive to the above-mentioned alteration processes. An annual growth increment

formation in the concave bands during winter, rarely spring, is in accordance with the investigations of Kirby (2000) in *Crassostrea gigantissima*. In contrast, Kirby et al. (1998) observed growth increment formation also during summer in *Crassostrea virginica* and interpreted these to reflect growth cessation due to high water temperatures (see also Lawrence 1988; Andrus and Crowe 2000).

In contrast to the ligament area, the inner ostracum is unsuitable for age estimations based on microstructure alterations. Comparing the alternation of the vesicular/foliate microstructure with the stable isotope record shows that the microstructure changed several times in certain years (Fig. 5b; e.g., years 1969, 1972) but was continuous in others (Fig. 5b; e.g., years 1963, 1974). This seriously compromises estimating ages by counting the microstructural changes. Andrus and Crowe (2000) observed comparable intra-annual changes in the microstructure of *Crassostrea virginica* and interpreted these as response to environmental stress, such as extreme temperatures or rain floods. The reasons for the microstructural changes in the inner ostracum of *H. hyotis* remain unclear. No link to flood events (by a comparison with rainfall data, not shown) is evident.

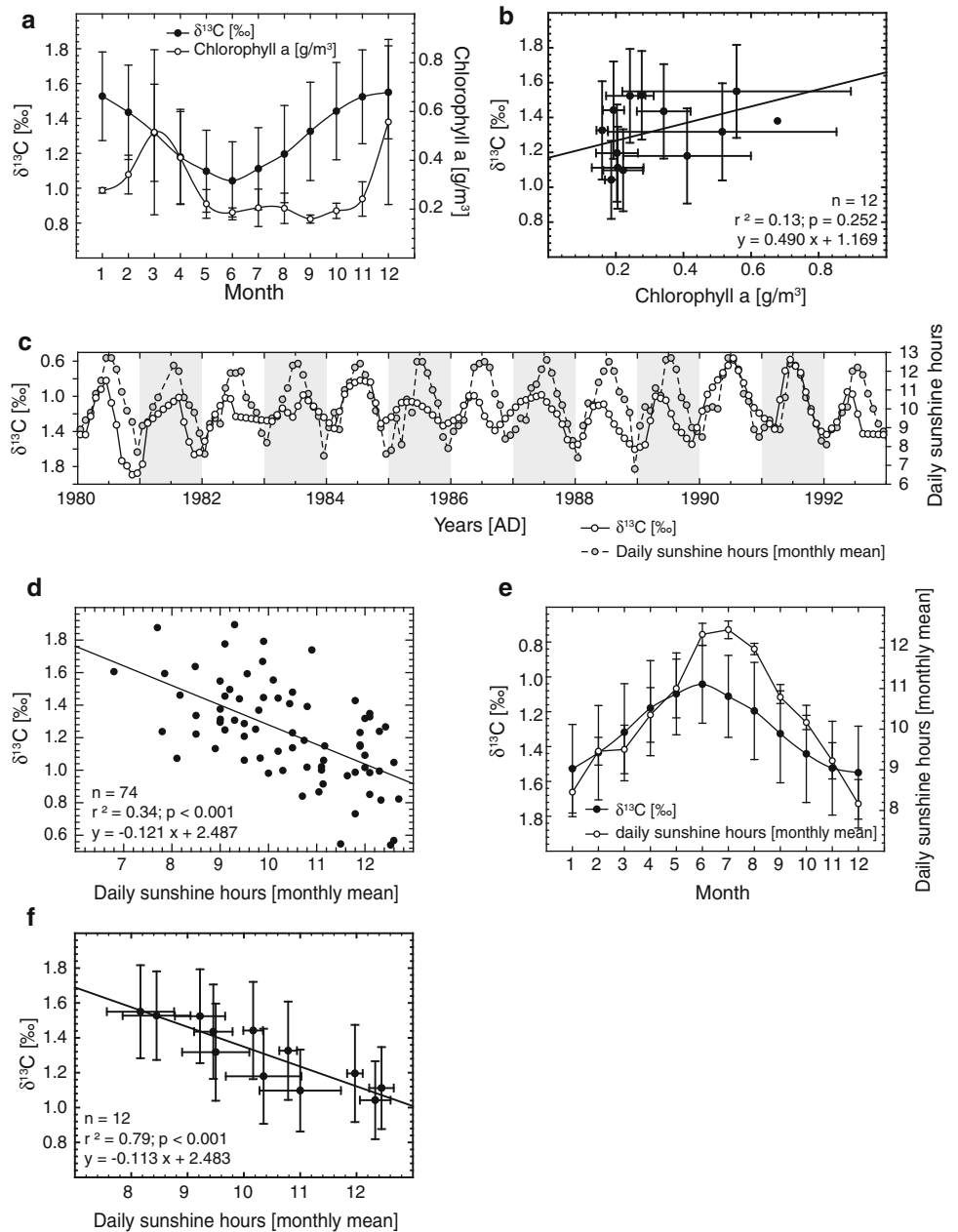
The estimated growth rates within the inner ostracum suggest increased growth rates (max. 3.3 mm/year) during the early ontogenetic stage (1958–1977), but decreased rates afterwards (Fig. 5c). This is in accordance with growth rates from other bivalves (Johnson et al. 2000; Kennedy et al. 2001; Richardson et al. 2004; Schöne et al. 2003b, 2004; Nakashima et al. 2004), including oysters (Kirby et al. 1998).

Stable isotopes

The partitioning of oxygen and carbon isotopes between seawater and biogenic carbonate depends on a variety of environmental parameters including temperature, isotopic composition of the water, primary production, atmospheric CO_2 concentration, and, unfortunately, also on biological (disequilibrium) fractionation processes known as ‘vital effects’ (McConnaughey 1989, 2003; McConnaughey and Gillikin 2008; Lartaud et al. 2010b). Two types of ‘vital effects’ are differentiated, kinetic and metabolic effects. A high correlation between $\delta^{18}\text{O}$ and $\delta^{13}\text{C}$ is generally regarded as strongly indicating a kinetic isotope effect (McConnaughey 1989; Omata et al. 2005). Metabolic processes exclusively affect the $\delta^{13}\text{C}$ signal (Lorrain et al. 2004; Omata et al. 2005).

Isotopic data of the studied oyster show low correlation between $\delta^{18}\text{O}$ and $\delta^{13}\text{C}$ (Fig. 6a), ruling out a significant kinetic fractionation. The $\delta^{18}\text{O}_{\text{oyster}}$ fluctuations are thus most likely controlled by the local SST variability, which is also suggested by the strong negative correlation between the two datasets (Fig. 7a, c; McConnaughey 1989; Omata et al. 2005).

Fig. 9 **a, b** Comparison of the mean values of every month for all years of the interpolated $\delta^{13}\text{C}_{\text{oyster}}$ record versus the chlorophyll a concentration. Note that there is no time overlap between $\delta^{13}\text{C}_{\text{oyster}}$ and the chlorophyll a data. **c** Plot of $\delta^{13}\text{C}_{\text{oyster}}$ and monthly mean daily sunshine hours. **d** Crossplot of daily sunshine and $\delta^{13}\text{C}_{\text{oyster}}$. **e** Mean values of every month for all years of interpolated $\delta^{13}\text{C}_{\text{oyster}}$ and daily sunshine hours. Both datasets show cyclic oscillations and are in-phase. **f** Crossplot of daily sunshine hours and $\delta^{13}\text{C}_{\text{oyster}}$ (mean values of every month of all years). Vertical, shaded bars indicate uneven years



There is no relationship between microstructure type and isotopic composition (Fig. 6a). This suggests that precipitation of a specific microstructure was not restricted to a particular season of the year and that biologically induced fractionation processes between the two microstructures were minor, in contrast to other oysters (Wisshak et al. 2009). This conclusion is supported by the fact that, in some years, several microstructure alternations occur and in others none (Fig. 5b).

Oxygen isotope record

The sinusoidal $\delta^{18}\text{O}_{\text{oyster}}$ oscillations are attributed to annual changes of environmental parameters including SST and the

isotopic composition of the seawater, which depends highly on the degree of evaporation (also expressed as changes in SSS; Fig. 3). Freshwater influence can be neglected because rainfall here is minimal (Awad et al. 1996). Best fit between the $\delta^{18}\text{O}_{\text{oyster}}$ and $\delta^{18}\text{O}_{\text{predicted}}$ (calculated from the SST using Eq. 4 of Wanamaker et al. 2007) was achieved using a $\delta^{18}\text{O}_{\text{seawater}}$ value of 2.17‰ (Fig. 8a, b). The maximal absolute error between the two records still reached 0.95‰. Potential methodological sources for the deviation between the $\delta^{18}\text{O}_{\text{oyster}}$ and the $\delta^{18}\text{O}_{\text{predicted}}$ signal are the sample resolution and sampling technique. Generally, the $\delta^{18}\text{O}_{\text{oyster}}$ amplitude is smaller than that of $\delta^{18}\text{O}_{\text{predicted}}$ (Figs. 7b, 8a). This might be an artefact of sample resolution. The sample

track distance of 270 μm might cause a minor smoothing (the environmental extremes might be recorded between the sample positions). Moreover, track length and positioning might influence the time averaging of the samples. In years of reduced growth, this time-averaging effect is further increased and, consequently, yields an even stronger artificial attenuation of maximum and minimum temperatures (Richardson 2001). The $\delta^{18}\text{O}_{\text{oyster}}$ values higher (1958–1962) and lower (1968–1973) than expected from the $\delta^{18}\text{O}_{\text{predicted}}$ record occur prior to 1977 where the oyster exhibits a generally increased growth rate (Figs. 5c, 8a). This suggests reduced time averaging by sampling during intervals of high shell growth and the most likely capture of local environmental extremes during these periods.

Alternatively, specific environmental conditions in Safaga Bay could partly or completely explain the observed discrepancies, especially the generally reduced amplitude. Salinity measurements in Safaga Bay in June 2001 yielded a mean value of $41.5 \pm 1\%$ (Helal and El-Wahab 2004). Piller and Pervesler (1989) even reported maximum salinities of 45‰ during summer here. Both measurements suggest maximal salinities in summer and contradict the CARTON-GIESE SODA version 2.0.2-4 dataset; that dataset points to highest salinities of 39.8‰ during winter for the open Red Sea close to Safaga Bay (Fig. 3b). According to LeGrande and Schmidt's (2006) $\delta^{18}\text{O}_{\text{seawater}}$ –salinity relationship for the Red Sea, higher salinities result in heavier $\delta^{18}\text{O}_{\text{seawater}}$ values. Consequently, high winter salinities would increase the amplitude of a $\delta^{18}\text{O}$ record, while high summer salinities would decrease it. The latter case, as suggested by direct SSS measurements, might explain the generally reduced $\delta^{18}\text{O}_{\text{oyster}}$ record. Intervals with an enhanced $\delta^{18}\text{O}_{\text{oyster}}$ amplitude might be caused by a flushing of Safaga Bay with open Red Sea waters in these years. Support for a significant difference between the local water mass in Safaga Bay and the open Red Sea surface water is also provided by the observation that the $\delta^{18}\text{O}_{\text{predicted}}$ calculated with a constant $\delta^{18}\text{O}_{\text{seawater}}$ value show a better fit with the $\delta^{18}\text{O}_{\text{oyster}}$ than the $\delta^{18}\text{O}_{\text{predicted}}$ with $\delta^{18}\text{O}_{\text{seawater(SSS)}}$ values calculated from the SSS record (Table 1; Fig. 8), which suggests that the salinity variations in Safaga Bay differ significantly from the open Red Sea salinity fluctuations. The weak correlation between $\delta^{18}\text{O}_{\text{oyster}}$ and the SSS (Fig. 7d–f) is best explained by the weak negative correlation between the open Red Sea SSS and the SST record in general ($r^2 = 0.26$, $P < 0.001$, $n = 460$; monthly mean values: $r^2 = 0.95$, $P < 0.001$, $n = 12$; both comparisons are not shown).

The herein-used $\delta^{18}\text{O}_{\text{seawater}}$ value of 2.17‰ is 0.3–0.8‰ higher than published $\delta^{18}\text{O}_{\text{seawater}}$ values from the region (1.85–1.36‰ at 27°N 34°W; Andrié and Merlivat 1989; Gansen and Kroon 1991). The increased evaporation (as already suggested) and reduced exchange with open Red Sea

surface waters no doubt increased the $\delta^{18}\text{O}_{\text{seawater}}$ value. According to LeGrande and Schmidt (2006), a 1‰ increase in salinity corresponds to a 0.31‰ increase in $\delta^{18}\text{O}_{\text{seawater}}$ in the Red Sea. Hence, the suggested 0.3–0.8‰ increase in $\delta^{18}\text{O}_{\text{seawater}}$ translates into a salinity increase of about 1.0–2.6‰ in Safaga Bay. The highest open Red Sea surface salinities are 1.7–5.2‰ lower than in Safaga (Piller and Pervesler 1989; Helal and El-Wahab 2004). Consequently, a heavier $\delta^{18}\text{O}_{\text{seawater}}$ of 2.17‰ is a reasonable estimate for the Safaga Bay surface waters. More direct measurements of the local temperature and salinity would help to unambiguously settle the $\delta^{18}\text{O}_{\text{seawater}}$ influence on the oxygen isotope record of *H. hyotis*.

Carbon isotope record

The carbon isotopic composition of skeletons of marine organisms varies in a more complex fashion than $\delta^{18}\text{O}$, and the origin of this variability is not fully understood (Lorrain et al. 2004). In principle, the $\delta^{13}\text{C}$ signal of shells is controlled by the $\delta^{13}\text{C}$ value of the dissolved inorganic carbon (DIC) of the organism's extrapallial fluid (EPF), from which the shell is precipitated (Kirby 2000). In (marine) bivalves, the carbon isotope composition of the EPF is controlled by the $\delta^{13}\text{C}$ of the ambient seawater, carbonate ion effects, pH, food availability, growth, valve gape/closure intervals, and seasonal changes in the metabolic rate (Romanek et al. 1992; McConnaughey et al. 1997; Kirby et al. 1998; Owen et al. 2002; McConnaughey 2003; Geist et al. 2005; McConnaughey and Gillikin 2008; Lartaud et al. 2010b). All these processes vary in strength and time, which complicates interpretation of the $\delta^{13}\text{C}$ signal (Lorrain et al. 2004; Omata et al. 2005).

The comparison of the $\delta^{13}\text{C}_{\text{oyster}}$ record with the chlorophyll a data suggests a depletion of the $\delta^{13}\text{C}_{\text{oyster}}$ at the start of planktonic blooms (Fig. 9; note, however, the insignificant, low correlation). The monthly mean daily sunshine hours are clearly in-phase and negatively correlated with the $\delta^{13}\text{C}_{\text{oyster}}$ record (Fig. 9). Both observations suggest that the $\delta^{13}\text{C}_{\text{oyster}}$ is most likely controlled by bivalve respiration, which is increased during periods of enhanced planktonic food supply (as indicated by increased chlorophyll a concentrations and increased daily sunshine hours). A similar process, causing a shift of up to 2‰, was already suggested by Owen et al. (2002) and Geist et al. (2005; see also Lorrain et al. 2004; Gillikin et al. 2007). This interpretation, however, remains speculative until supported by on-site environmental data.

Giant oysters as potential environmental archives in coral reefs

This study provides the first decadal oxygen and carbon isotope record of the giant oyster *H. hyotis*. The studied

specimen was about 40 years old when sampled. Its lifespan was estimated by counting the concave–convex growth bands on the ligament surface, although alteration processes, such as abrasion or bioerosion, can reduce reliability.

The $\delta^{18}\text{O}$ record is strongly correlated with the SST. The significant higher estimated $\delta^{18}\text{O}_{\text{seawater}}$ value, compared to open Red Sea conditions, most likely reflect the specific seawater conditions in the semi-enclosed coastal Safaga Bay embayment. Specific nearshore seawater conditions might also explain the discrepancies of up to 0.95‰ between the $\delta^{18}\text{O}_{\text{oyster}}$ and $\delta^{18}\text{O}_{\text{predicted}}$, calculated from the SST record with an $\delta^{18}\text{O}_{\text{seawater}}$ value of 2.17‰. Direct salinity measurements in the bay suggest maximal values of 45‰ during summer, whereas salinity in the open Red Sea surface water peaks during winter (39.8‰). Finally, sample resolution, drilling track length, and track position might add to the large absolute error of individual measurements. When comparing the mean monthly values, however, the temperature discrepancies between reconstructed and global grid datasets always remain $<1.0^\circ\text{C}$. The $\delta^{13}\text{C}$ signal is interpreted to reflect mainly changes in the respiration rate.

The calcitic mineralogy, fixosessile lifestyle, and long lifespan make this oyster a promising environmental archive in Indo-Pacific coral reefs. The oyster seems to precipitate its shell in isotopic equilibrium with the seawater and provides a promising archive for ancient SSTs and SSSs. In the fossil record, particular attention should be paid to the sedimentological context, and the palaeogeographic position of specimens. Results based on fossils from partly enclosed coastal embayments might significantly depart from open oceanographic conditions, as exemplified in this study. Data from such environments should be avoided by climate modellers.

Acknowledgments Manuela Wimmer is thanked for assistance in the isotope laboratory. Max Wisshak and Matthias López Correa (both GeoZentrum Nordbayern), and Henning Kuhnert and Thomas Felis (both University Bremen) are gratefully acknowledged for fruitful discussions. We thank Michael Stachowitsch (University Vienna) for useful comments on a late version of the manuscript. Chris Romanek and an anonymous reviewer provided constructive reviews.

References

- Aharon P (1991) Records of reef environment histories: stable isotopes in corals, giant clams, and calcareous algae. *Coral Reefs* 10:71–90
- Ahmed F, Sultan SAR (1987) On the heat balance terms in the central region of the Red Sea. *Deep-Sea Res* 34:1757–1760
- Al-Rousan S, Al-Moghrabi S, Pätzold J, Wefer G (2002) Environmental and biological effects on the stable isotope records of corals in the northern Gulf of Aqaba, Red Sea. *Mar Ecol Prog Ser* 239:301–310
- Anderson TF, Arthur MA (1983) Stable isotopes of oxygen and carbon and their application to sedimentologic and paleoenvironmental problems. *SEPM Short Course* 10:1–151
- Andrié C, Merlivat L (1989) Contribution des données isotopiques de deutérium, oxygène-18, hélium-3 et tritium, à l'étude de la circulation de la Mer Rouge. *Oceanol Acta* 12:165–174
- Andrus CFT, Crowe DE (2000) Geochemical analysis of *Crassostrea virginica* as a method to determine season of capture. *J Archaeol Sci* 27:33
- Awad MA, Hamza MS, Atwa SM, Sallouma MK (1996) Isotopic and hydrogeochemical evaluation of groundwater at Qusier-Safaga area, eastern desert, Egypt. *Environ Geochem Health* 18:47–54
- Bieler R, Mikkelsen PM, Lee T, Foighil DÓ (2004) Discovery of the Indo-Pacific oyster *Hyotissa hyotis* (Linnaeus, 1758) in the Florida Keys (Bivalvia: Gryphaeidae). *Molluscan Res* 24:149–159
- Butler PG, Richardson CA, Scourse JD, Witbaard R, Schöne BR, Fraser NM, Wanamaker AD, Bryant CL, Harris I, Robertson I (2009a) Accurate increment identification and the spatial extent of the common signal in five *Arctica islandica* chronologies from the Fladen Ground, northern North Sea. *Paleoceanography* 24. doi:10.1029/2008PA001715
- Butler PG, Scourse JD, Richardson CA, Wanamaker AD Jr, Bryant CL, Bennell JD (2009b) Continuous marine radiocarbon reservoir calibration and the ^{13}C Suess effect in the Irish Sea: Results from the first multi-centennial shell-based marine master chronology. *Earth Planet Sci Lett* 279:230–241
- Carré M, Bentaleb I, Blamart D, Ogle N, Cardenas F, Zevallós S, Kalin RM, Orlieb L, Fontugne M (2005) Stable isotopes and sclerochronology of the bivalve *Mesodesma donacium*: Potential application to Peruvian paleoceanographic reconstructions. *Palaeogeogr Palaeoecol* 228:4–25
- Carton JA, Giese BS (2008) A reanalysis of ocean climate using SODA. *Mon Weather Rev* 136:2999–3017
- Crame JA (1986) Late Pleistocene molluscan assemblages from the coral reefs of the Kenya coast. *Coral Reefs* 4:183–196
- Dunca E, Schöne BR, Mutvei H (2005) Freshwater bivalves tell of past climates: But how clearly do shells from polluted rivers speak? *Palaeogeogr Palaeoecol* 228:43–57
- Edwards FJ (1987) Climate and oceanography. In: Edwards AJ, Head ST (eds) Key environments. Red Sea. Pergamon Press, Oxford, pp 45–69
- Elliot M, Welsh K, Chilcott C, McCulloch M, Chappell J, Ayling B (2009) Profiles of trace elements and stable isotopes derived from giant long-lived *Tridacna gigas* bivalves: Potential applications as palaeoclimate studies. *Palaeogeogr Palaeoecol* 208:132–142
- Eshel G, Heavens N (2007) Climatological evaporation seasonality in the northern Red Sea. *Paleoceanography* 22: PA42109, 1–15
- Felis T, Lohmann G, Kuhnert H, Lorenz SJ, Scholz D, Pätzold J, Al-Rousan SA, Al-Moghrabi SM (2004) Increased seasonality in Middle East temperatures during the last interglacial period. *Nature* 429:164–168
- Gansen G, Kroon D (1991) Evidence for Red Sea circulation from O isotopes of modern surface waters and planktonic foraminiferal test. *Paleoceanography* 6:73–82
- Geist J, Auerswald K, Boom A (2005) Stable carbon isotopes in freshwater mussel shells: Environmental record or marker for metabolic activity? *Geochim Cosmochim Acta* 69:3545–3554
- Gillikin DP, De Ridder F, Ulens H, Elskens M, Keppens E, Baeyens W, Dehairs F (2005) Assessing the reproducibility and reliability of estuarine bivalve shells (*Saxidomus giganteus*) for sea surface temperature reconstruction: Implications for paleoclimate studies. *Palaeogeogr Palaeoecol* 228:70–85

- Gillikin DP, Lorrain A, Meng L, Dehairs F (2007) A large metabolic carbon contribution to the $\delta^{13}\text{C}$ record in marine aragonitic bivalve shells. *Geochim Cosmochim Acta* 71:2936–2946
- Goman M, Ingram BL, Strom A (2008) Composition of stable isotopes in geoduck (*Panopea abrupta*) shells: A preliminary assessment of annual and seasonal paleoceanographic changes in the northeast Pacific. *Quaternary Int* 188:117–125
- Grill B, Zuschin M (2001) Modern shallow- to deep-water bivalve death assemblages in the Red Sea—ecology and biogeography. *Palaeogeogr Palaeoecol* 168:75–96
- Helal SA, El-Wahab HA (2004) Recent ostracodes from marine sediments of Safaga Bay, Red Sea, Egypt. *Egypt J Paleontol* 4:75–93
- Hickson JA, Johnson ALA, Heaton THE, Balson PS (1999) The shell of the Queen Scallop *Aequipecten opercularis* (L.) as a promising tool for palaeoenvironmental reconstruction: evidence and reasons for equilibrium stable-isotope incorporation. *Palaeogeogr Palaeoecol* 154:325–337
- Hong W, Keppens E, Nielsen P, van Riet A (1995) Oxygen and carbon isotope study of the Holocene oyster reefs and palaeoenvironmental reconstruction on the northwest coast of Bohai Bay, China. *Mar Geol* 124:289–302
- Johnson ALA, Hickson JA, Swan J, Brown MR, Heaton THE, Chenery S, Balson PS (2000) The queen scallop *Aequipecten opercularis*: a new source of information on late Cenozoic marine environments in Europe. In: Harper EM, Taylor JD, Crame JA (eds) *The evolutionary biology of the Bivalvia*. *Geol Soc London Spec Publ* 177:425–439
- Jones DS, Williams DF, Romanek CS (1986) Life history of symbiont-bearing giant clams from stable isotope profiles. *Science* 231:46–48
- Jones DS, Arthur MA, Allard DJ (1989) Sclerochronological records of temperature and growth form shells of *Mercenaria mercenaria* from Narragansett Bay, Rhode Island. *Mar Biol* 102:225–234
- Kennedy H, Richardson CA, Duarte CM, Kennedy DP (2001) Oxygen and carbon stable isotopic profiles of the fan mussel, *Pinna nobilis*, and reconstruction of sea surface temperatures in the Mediterranean. *Mar Biol* 139:1115–1124
- Kirby MX (2000) Paleocological differences between Tertiary and Quaternary *Crassostrea* oysters, as revealed by stable isotope sclerochronology. *Palaios* 15:132–141
- Kirby MX, Soniat TM, Spero HJ (1998) Stable isotope sclerochronology of Pleistocene and Recent oyster shells (*Crassostrea virginica*). *Palaios* 13:560–569
- Klein R, Tudhope AW, Chilcott CP, Pätzold J, Abdulkarim Z, Fine M, Fallick AE, Loya Y (1997) Evaluating southern Red Sea corals as a proxy record for the Asian monsoon: *Earth Planet Sci Lett* 148:381–394
- Krantz DE, Williams DF, Jones DS (1987) Ecological and palaeoenvironmental information using stable isotope profiles from living and fossil molluscs. *Palaeogeogr Palaeoecol* 58:249–266
- Lartaud F, Emmanuel L, De Rafelis M, Ropert M, Labourdette N, Richardson CA, Renard M (2010a) A latitudinal gradient of seasonal temperature variation recorded in oyster shells from the coastal waters of France and The Netherlands. *Facies* 56:13–25
- Lartaud F, Emmanuel L, De Rafelis M, Pouvreau S, Renard M (2010b) Influence of food supply on the $\delta^{13}\text{C}$ signature of mollusc shells: implications for palaeoenvironmental reconstructions. *Geo-Mar Lett* 30:23–34
- Lawrence DR (1988) Oysters as geoarchaeologic objects. *Geoarchaeology* 3:267–274
- LeGrande AN, Schmidt GA (2006) Global gridded data set of oxygen isotopic composition in seawater. *Geophys Res Lett* 33: L12604, 1–5
- Lietard C, Pierre C (2008) High-resolution isotopic records ($\delta^{18}\text{O}$ and $\delta^{13}\text{C}$) and cathodoluminescence study of lucinid shells from methane seeps of the Eastern Mediterranean. *Geo-Mar Lett* 28:195–203
- Lorrain A, Paulet Y-M, Chauvaud L, Dunbar R, Mucciarone D, Fontugne M (2004) $\delta^{13}\text{C}$ variations in scallop shells: Increasing metabolic carbon contribution with body size? *Geochim Cosmochim Acta* 68:3509–3519
- McConnaughey T (1989) ^{13}C and ^{18}O isotopic disequilibrium in biologic carbonates: II. In vitro simulation of kinetic isotope effects. *Geochim Cosmochim Acta* 53:163–171
- McConnaughey TA (2003) Sub-equilibrium oxygen-18 and carbon-13 levels in biological carbonates: carbonate and kinetic models. *Coral Reefs* 22:316–327
- McConnaughey T, Gillikin DP (2008) Carbon isotopes in mollusk shell carbonates. *Geo-Mar Lett* 28:287–299
- McConnaughey TA, Burdett J, Whelan JF, Paull CK (1997) Carbon isotopes in biological carbonates: respiration and photosynthesis. *Geochim Cosmochim Acta* 61:611–622
- Medio D, Sheppard CRC, Gascoigne J (2000) The Red Sea. In: McClanahan TR, Sheppard CRC, Obdura DO (eds) *Coral reefs of the Indian Ocean*. Oxford University Press, Oxford, pp 231–255
- Nakashima R, Suzuki A, Watanabe T (2004) Life history of the Pliocene scallop *Fortipecten*, based on oxygen and carbon isotope profiles. *Palaeogeogr Palaeoecol* 211:299–307
- Omata T, Suzuki A, Kawahat H, Okamoto M (2005) Annual fluctuation in the stable carbon isotope ratio of coral skeletons: the relative intensities of kinetic and metabolic isotope effects. *Geochim Cosmochim Acta* 69:3007–3016
- Owen R, Kennedy H, Richardson C (2002) Experimental investigation into partitioning of stable isotopes between scallop (*Pecten maximus*) shell calcite and sea water. *Palaeogeogr Palaeoecol* 185:163–174
- Piller WE, Pervesler P (1989) The Northern Bay of Safaga (Red Sea, Egypt): an actuopalaeontological approach. *Beitr Paläont Österreicher* 15:103–147
- Putten EV, Dehairs F, Keppens E, Baeyens W (2000) High resolution distribution of trace elements in the calcite shell layer of modern *Mytilus edulis*: environmental and biological controls. *Geochim Cosmochim Acta* 64:997
- Richardson CA (2001) Molluscs as archives of environmental change. *Oceanogr Mar Biol Annu Rev* 39:103–164
- Richardson CA, Peharda M, Kennedy H, Kennedy P, Onofri V (2004) Age, growth rate and season of recruitment of *Pinna nobilis* (L) in the Croatian Adriatic determined from Mg:Ca and Sr:Ca shell profiles. *J Exp Mar Biol Ecol* 299:1–16
- Riegl B, Piller WE (1997) Distribution and environmental control of coral assemblages in Northern Safaga Bay (Red Sea, Egypt). *Facies* 36:141–162
- Rimbu N, Felis T, Lohmann G, Pätzold J (2006) Winter and summer climate patterns in the European-Middle East during recent centuries as documented in a northern Red Sea coral record. *The Holocene* 16:321–330
- Romanek CS, Grossman EL (1989) Stable isotope profiles of *Tridacna maxima* as environmental indicators. *Palaios* 4:402–413
- Romanek CS, Grossman EL, Morse JW (1992) Carbon isotopic fractionation in synthetic aragonite and calcite—Effects of temperature and precipitation rate. *Geochim Cosmochim Acta* 56:419–430
- Schöne BR (2003) A ‘clam-ring’ master-chronology constructed from a short-lived bivalve mollusc from the northern Gulf of California, USA. *The Holocene* 13:39–49
- Schöne BR, Lega J, Flessa KW, Goodwin DH, Dettman DL (2002) Reconstructing daily temperatures from growth rates of the intertidal bivalve mollusk *Chione cortezi* (northern Gulf of California, Mexico). *Palaeogeogr Palaeoecol* 184:131–146

- Schöne BR, Oschmann W, Kröncke I, Dreyer W, Janssen R, Rumohr H, Houk SD, Freyre Castro AD, Dunca E, Rössler J (2003a) North Atlantic Oscillation dynamics recorded in shells of a long-lived bivalve mollusk. *Geology* 31:1237–1240
- Schöne BR, Tanabe K, Dettman DL, Sato S (2003b) Environmental controls on shell growth rates and $\delta^{18}\text{O}$ of the shallow-marine bivalve mollusc *Phacosoma japonicum* in Japan. *Mar Biol* 142:473–485
- Schöne BR, Freyre Castro AD, Fiebig J, Houk SD, Oschmann W, Kröncke I (2004) Sea surface water temperatures over the period 1884–1983 reconstructed from oxygen isotope ratios of a bivalve mollusk shell (*Arctica islandica*, southern North Sea). *Palaeogeogr Palaeoecol* 212:215–232
- Schöne BR, Dunca E, Mutvei H, Baier S, Fiebig J (2005a) Scandinavian climate since the late 18th century reconstructed from shells of bivalve mollusks. *Z Dtsch Ges Geowiss* 156:501–516
- Schöne BR, Fiebig J, Pfeiffer M, Gleß R, Hickson JA, Johnson ALA, Dreyer W, Oschmann W (2005b) Climate records from a bivalved *Methuselah* (*Arctica islandica*, Mollusca; Iceland). *Palaeogeogr Palaeoecol* 228:130–148
- Scourse J, Richardson C, Forsythe G, Harris I, Heinemeier J, Fraser N, Briffa K, Jones P (2006) First cross-matched floating chronology from the marine fossil record: data from growth lines of the long-lived bivalve mollusc *Arctica islandica*. *The Holocene* 16:967–974
- Spötl C, Vennemann T (2003) Continuous-flow IRMS analysis of carbonate minerals. *Rapid Commun Mass Spectrom* 17:1004–1006
- Strom A, Francis RC, Mantua NJ, Miles EL, Peterson DL (2005) Preserving low-frequency climate signals in growth records of geoduck clams (*Panopea abrupta*). *Palaeogeogr Palaeoecol* 228:167–178
- Surge D, Walker KJ (2006) Geochemical variation in microstructural shell layers of the southern quahog (*Mercaenaria campechiensis*): Implications for reconstructing seasonality. *Palaeogeogr Palaeoecol* 237:182–190
- Surge DM, Lohmann KC, Dettman DL (2001) Controls on isotopic chemistry of the American oyster, *Crassostrea virginica*: implications for growth patterns. *Palaeogeogr Palaeoecol* 172:283–296
- Surge DM, Lohmann KC, Goodfriend GA (2003) Reconstructing estuarine conditions: oyster shells as recorders of environmental change, Southwest Florida. *Estuar Coast Shelf Sci* 57:737–756
- Takesue RK, van Geen A (2004) Mg/Ca, Sr/Ca, and stable isotopes in modern and Holocene *Protothaca staminea* shells from a northern California coastal upwelling region. *Geochim Cosmochim Acta* 68:3845–3861
- UK Meteorological Office, Hadley Centre (2006) HadISST 1.1—Global Sea-Ice coverage and SST (1870–Present), British Atmospheric Data Centre
- Wanamaker AD Jr, Kreutz KJ, Borns Jr HW, Introne DS, Feindel SC, Funder S, Rawson PD, Barber BJ (2007) Experimental determination of salinity, temperature, growth, and metabolic effects on shell chemistry of *Mytilus edulis* collected from Maine and Greenland. *Paleoceanography* 22:PA2217, 1–12
- Wanamaker AD Jr, Heinemeier J, Scourse JD, Richardson CA, Butler PG, Eriksson J, Knudsen KL (2008a) Very long-lived mollusks confirm 17th century AD tephra-based radiocarbon reservoir ages from north Icelandic shelf waters. *Radiocarbon* 50:399–412
- Wanamaker AD Jr, Kreutz KJ, Schöne BR, Pettigrew N, Borns HW, Introne DS, Belknap D, Maasch KA, Feindel S (2008b) Coupled North Atlantic slope water forcing on Gulf of Maine temperatures over the past millennium. *Clim Dynam* 31:183–194
- Watanabe T, Oba T (1999) Daily reconstruction of water temperature from oxygen isotopic ratios of a modern *Tridacna* shell using a freezing microtome sampling technique. *J Geophys Res-Oceans* 104:20667–20674
- Watanabe T, Suzuki A, Kawahata H, Kan H, Ogawa S (2004) A 60-year isotopic record from a mid-Holocene fossil giant clam (*Tridacna gigas*) in the Ryukyu Islands: physiological and paleoclimatic implications. *Palaeogeogr Palaeoecol* 212:343–354
- Wisshak M, López Correa M, Gofas S, Salas C, Taviani M, Jakobsen J, Freiwald A (2009) Shell architecture, element composition, and stable isotope signature of the giant deep-sea oyster *Neopycnodonte zibrowii* sp.n. from the NE Atlantic. *Deep-Sea Res I* 56:374–407
- Zuschin M, Baal C (2007) Large gryphaeid oysters as habitats for numerous sclerobionts: a case study from the northern Red Sea. *Facies* 53:319–327
- Zuschin M, Hohenegger J (1998) Subtropical coral-reef associated sedimentary facies characterized by molluscs (Northern Bay of Safaga, Red Sea, Egypt). *Facies* 38:229–254
- Zuschin M, Oliver PG (2003a) Bivalves and bivalve habitats in the northern Red Sea. Verlag des Naturhistorischen Museums, Wien
- Zuschin M, Oliver PG (2003b) Fidelity of molluscan life and death assemblages on sublittoral hard substrata around granitic islands of the Seychelles. *Lethaia* 36:133–149
- Zuschin M, Hohenegger H, Steininger FF (2001) Molluscan assemblages on coral reefs and associated hard substrata in the northern Red Sea. *Coral Reefs* 20:107–116